Journal of the Mechanical Behavior of Biomedical Materials 181 (2026) 107507

Contents lists available at ScienceDirect

Journal of the Mechanical Behavior of Biomedical Materials

journal homepage: www.elsevier.com/locate/jmbbm

Use of indentation test methods for additive manufacturing build verification for Ti-6Al-4V

Abigail Tetteh [a], Daniel Porter [a], Thomas Southern [b], Jimmy Campbell [b], Mary Fortune [c], Matthew Di Prima [a,*]

[a] Division of Applied Mechanics, Office of Science and Engineering Laboratories, Center for Devices and Radiological Health, United States Food and Drug Administration, Silver Spring, MD, 20993, USA
[b] Plastometrex, Cambridge Technopark, Newmarket Rd, Cambridge, CB5 8PB, UK
[c] Department of Public Health and Primary Care, University of Cambridge, Forvie Site, Robinson Way, Cambridge, CB2 0SR, UK

ARTICLE INFO

Keywords:
Additive manufacturing
Microhardness
Mechanical property
Tensile strength
Profilometry indentation plastometry

ABSTRACT

Additive Manufacturing (AM), commonly called 3D printing, has increased significantly for medical device production since 2010. Despite ongoing technological improvements, the variability of mechanical properties for AM parts tends to exceed the variability in parts built using traditional manufacturing techniques. To assess this variability, the current approach is to perform tensile tests to verify the mechanical performance of each build. While this approach has a long history of use, tensile coupons are often taller than the devices being produced, which leads to longer build times to account for the additional height and potentially the need to machine these coupons before testing. While several AM build verification approaches have been proposed, this effort focuses on assessing a traditional indentation technique (Vickers micro-hardness) with a new indentation technique based on plastometry, Profilometry-based Indentation Plastometry (PIP), which is cost effective and time efficient. AM and conventional wrought titanium alloy tensile coupons (per ASTM E8) were obtained from multiple vendors and tested. After testing, indentation coupons were cut from the grip sections of the tensile coupons. Vickers and PIP testing were then conducted to obtain the most accurate comparison between tensile and indentation results. A linear regression analysis was performed to evaluate the two indentation methods and their feasibility for build verification by comparing their results to tensile test outcomes. While there were a few outliers, attributed to anisotropy in those samples, the correlation between measured tensile results and those predicted by PIP was similar for the AM and wrought specimens for yield strength (0.48 and 0.22) and ultimate tensile strength (0.85 and 0.84), respectively. Measurements predicted from Vickers micro-hardness showed a better correlation to the measured tensile results for AM specimens than wrought, based on the coefficients of determination for yield strength (0.59 and 0.14) and ultimate tensile strength (0.70 and 0.17), respectively. These results indicate that, with sufficient validation, indentation techniques could be utilized in future AM build verification testing.

1. Introduction

Additive manufacturing (AM), commonly called 3D printing, has enabled innovation in design and fabrication in a wide range of applications. Due to the ease in the creation of complex structures, rapid prototyping, design-change capabilities, lightweighting, and customization, AM is increasingly being adopted in medical device fabrication (Karolewska et al., 2020; Hernandez-Nava et al., 2019; Fousova et al., 2018; Radlof et al., 2020). Unlike traditional or conventional manufacturing, such as forging, casting, and machining that require special molds, tools or dies to create wrought materials, AM enables the creation of parts directly into their near-final form (Fousova et al., 2018). From 2016 to 2020, about 68% of AM medical devices cleared by the FDA through the 510(k) process were made from Ti-6Al-4V (Ti6Al4V) alloy (Fogarasi et al., 2023), making it the most commonly used alloy for AM medical devices. Ti6Al4V alloy is widely used in

* Corresponding author. U.S. Food and Drug Administration, Center for Devices and Radiological Health, 10903 New Hampshire Ave., WO62-2215, Silver Spring, MD, 20993, USA.
E-mail address: matthew.diprima@fda.hhs.gov (M. Di Prima).

https://doi.org/10.1016/j.jmbbm.2026.107507
Received 20 February 2026; Received in revised form 21 May 2026; Accepted 16 June 2026
Available online 19 June 2026
1751-6161/Published by Elsevier Ltd.

orthopedic implant applications, both AM and traditionally manufactured, due to its strength, corrosion resistance, low density, and biocompatibility (Elias et al., 2008; Kaur and Singh, 2019).

Across the 7 types of AM techniques available (Additive manufacturing, 2021), there is a shared principle where material is deposited layer by layer to form a structure based on a digital design. The AM technology widely adopted to produce medical devices from the Ti6Al4V material is laser beam powder bed fusion (PBF-LB) (Hernandez-Nava et al., 2019). Common across PBF-LB systems is the wide disparity in manufacturing variables stemming from build parameters (scan speed, beam power, layer thickness), environmental parameters (oxygen level, pressure, temperature, gas flow characteristics), material parameters (melting temperature, heat of fusion, thermal conductivity, powder properties), and part parameters (size, bulkiness, downfacing areas, part orientation) (Fousova et al., 2018; de et al., 2023; Schwalbach et al., 2022; Hooreweder). Changes in these build parameters can result in significant changes to the material properties of the final printed component.

Before AM fabricated components are used for medical devices, their mechanical properties are evaluated to ensure they are suitable for the intended purpose per the manufacturer's quality management system (Lincoln, 2012). Performing tensile tests on representative specimens from various locations and orientations within a build, as well as under different conditions, can be costly and impractical when investigating the effects on mechanical properties (Southern et al., 2024). Although others have attempted to predict mechanical properties based on microstructural changes and phase compositions, these methods require comprehensive analyses of both the microstructure and chemical composition (Collins et al., 2009). In contrast, microhardness measurements and profilometry-based indentation plastometry (PIP) can be used as a more cost-effective and time-efficient alternative. The two tests are similar, in that an indenter is pressed into the surface of a material at a specified load and duration, followed by the measurement of the indentation to characterize the material's strength. The PIP test includes two further steps which are measuring the profile of the indentation and utilizing iterative finite element method (FEM) simulations to determine the plasticity parameters of the material.

The use of hardness measurements as a predictive tool for mechanical property determination has been adopted for materials such as nickel (Ni), copper (Cu), iron (Fe), and aluminum (Al), and their alloys (Tekkaya, 2001; Cahoon et al., 1971; Tabor, 1951; Lai and Lim, 1991). However, studies report that applying this approach to Ti6Al4V poses a challenge due to its tendency to strain harden (Tabor, 1951). Southern et al. used hardness tests to model the stress-strain behavior of 12 different alloys and compared it with tensile test responses. The models were reasonably accurate for alloys that exhibited little to no work hardening, but less accurate for materials with work hardening tendencies (Southern et al., 2023). While these studies have made valuable contributions to the feasibility of using hardness-based measurements to predict mechanical properties, none of these studies investigated combined conventional Vickers microhardness and PIP tests on wrought and AM Ti6Al4V.

In this study, the PIP method was used to derive the yield and ultimate tensile strength of AM and wrought Ti6Al4V alloy specimens, which were previously tested in quasi-static uniaxial tension. Vickers microhardness testing was performed on the same specimens. The strength properties obtained from the PIP test were compared with the results of the tensile tests to assess the feasibility of the PIP method in predicting the material's mechanical properties and use for AM build verification. Additionally, the relationships between strength, hardness, and oxygen content were examined using linear regression analyses.

2. Methods and materials

2.1. Tensile testing

Uniaxial quasi-static tensile testing was performed in accordance with ASTM E8/E8M-16a (Standard Test Methods for Tension, 2016) on wrought Ti6Al4V and PBF-LB AM Ti6Al4V samples sourced from multiple vendors. The AM samples were built oversized to the ASTM specimen geometry and dimensions (round tension test specimen 4) by the vendors such that the tensile test direction would be parallel to the build direction. Gauge regions were later machined in-house to reduce the surface roughness of the specimens and to achieve the standard dimensions. The wrought samples were machined from 9.5 mm (3/8″) diameter drawn rods, maintaining their original outer diameter while reducing the gauge region to meet the same specified tensile test geometry. Wrought samples underwent annealing and AM samples underwent hot isostatic pressing (HIP) post-processing treatment. Specimens were randomized to avoid unintentional bias during testing. Tensile tests were carried out at room temperature using an Instron 68FM-100 Universal Testing System (Illinois Tool Works, Norwood, MA, USA), which was equipped with a 25.4 mm (1-inch) gauge Instron extensometer. Samples were tested under displacement control of the crosshead at a 2.5 mm/min speed. The collected data were analyzed with MATLAB (R2023a, MathWorks, Natick, MA, USA) software to extract Elastic modulus (E), Ultimate Tensile Strength (UTS), and 0.2% offset Yield Strength (YS).

2.2. Microhardness measurements

The Vickers hardness (HV) test was performed on the grip sections of the tensile specimens in accordance with ASTM E92-23 (Standard Test Methods for Vickers, 2023), with indentation parallel to the build direction. Ti6Al4V samples were sectioned on the Abrasimet™ M manual abrasive cutter (Buehler, Lake Bluff IL, USA), and embedded in epoxy composed of epokwick epoxy resin and epokwick epoxy hardener (Buehler, Lake Bluff IL, USA) in a Frekote 770-NC mold release (Loctite, Rocky Hill, CT) coated with Buehler SamplKups. The cured epoxy containing the embedded samples was then polished using the Polimet polisher (Beuhler, Lake Bluff, IL) with progressively finer grit size silicon carbide (SiC) abrasive paper until samples were smooth and free of striations.

The polished samples were indented with a 1 kgf diamond indenter at 10 s dwell time on a Wilson VH1202 micro hardness tester (Beuhler, Lake Bluff, IL, USA), using the Vickers geometry. The indent diagonals were measured with the built-in optical microscope. Multiple indentations ($n = 4$) were made per specimen.

2.3. Profilometry-based indentation plastometry (PIP) testing

The same set of samples tested for microhardness was sent to Plastometrex Ltd. (Cambridge, UK) for PIP testing. The samples were repolished, and the PIP testing was performed according to ASTM E3499-25 at room temperature, parallel to the build direction, using the PLX-Benchtop tester (Plastometrex, Cambridge, UK) at 1 μm/s speed to determine the mechanical behavior of the material. The surfaces of the samples were indented with a 0.5 mm radius spherical Si_3N_4 indenter at a specified force (1139 N), and the profiles of the indents were characterized with a profilometer at 1 μm resolution. Using pre-defined elastic constants such as elastic modulus (assumed at 115 GPa) and Poisson's ratio (assumed at 0.3) as input data, an iterative finite element analysis of the indentation was then used to find the best-fit set of plasticity parameters based on the Voce equation below. The analysis enables the approximation of parameters such as YS and UTS. The results obtained were compared with those from the uniaxial tensile testing.

$$\sigma = \sigma_s - (\sigma_s - \sigma_Y) exp\left(-\frac{\varepsilon}{\varepsilon_0}\right) \quad (1)$$

where σ_Y is the yield stress, σ_s is the saturation stress, and ε_0 is the characteristic strain. The result is the von mises stress (σ) and von mises equivalent plastic strain (ε). A more detailed description of the method has previously been explained (Southern et al., 2023; Tang et al., 2021) with further detail of the FEM process also provided in supplement S1.

One of the assumptions for the use of PIP is that the sample being tested is isotropic. This assumption, combined with the use of a spherical indenter results in radially symmetric indents. Indents into an anisotropic material result in radial asymmetry of the residual indent profile (Tang et al., 2021). Harder directions resist deformation more than softer directions, resulting in differences in the maximum pile up height as a function of angle around the indent. Typically, AM components show transverse isotropy; directions within the build plane show similar mechanical properties, while properties can differ perpendicular to the build plane. Select samples in this work were additionally indented perpendicular to the build direction to investigate the presence of any anisotropy.

2.4. Oxygen content

The oxygen contents of all wrought and AM Ti6Al4V samples (n = 3 – 4 each) were tested by IMR Test Labs (Curtiss-Wright Corporation, Lansing, NY, USA). Measurements were performed with an ONH836 Elemental Analyzer (Leco, St. Joseph, MI, USA) according to the ASTM E1409-13 (Standard Test Method for Determination, 2013). The oxygen content results were used to verify any correlations between tensile test results with respect to the PIP and microhardness measurements.

2.5. Data analyses

Initial data processing and the calculation of mean absolute percentage errors (MAPE) were done using Microsoft Excel (Redmond, Washington, USA). Statistical analyses for comparing sample groups were performed in GraphPad Prism 8.4.3 software (San Diego, California, USA). The Shapiro-Wilk test was used to assess the data's normality. The Mann-Whitney test was used to compare all the tensile properties between AM and wrought Ti6Al4V samples, as well as to compare their tensile strengths obtained from the PIP and tensile tests. Microhardness values between AM and wrought samples were compared using an unpaired *t*-test. The Spearman correlation test was also used to evaluate the relationship between their oxygen content and tensile strengths.

Regression analysis was performed in R Version 4.4.3 software (Faraway, 2002). Linear regression models were fitted to evaluate the relationship between tensile testing values and both PIP and hardness testing for UTS and YS of AM and wrought samples. These models omitted five samples showing significant anisotropy, as PIP modeling assumes isotropy. Based on these models, coefficients of determination were calculated to quantify the correlation between the two techniques. 95% confidence intervals and prediction intervals were calculated to quantify the uncertainty in the estimate of the relationship.

3. Results

3.1. Mechanical properties of AM and wrought

The tensile mechanical properties, including elastic modulus (E), yield strength (YS), and ultimate tensile strength (UTS), were determined for both wrought and AM as shown in Table 1. The E of AM samples were significantly higher (135 ± 10.6 GPa) compared with the wrought samples (117 ± 7.3 GPa: $p < 0.001$). Conversely, YS and UTS were significantly higher in the wrought samples (1000 ± 39.4 MPa, 1080 ± 40.9 MPa, respectively) than in the AM samples (942 ± 66.3 MPa: $p = 0.004$, 1026 ± 48.0 MPa: $p < 0.001$, respectively).

The HVs of the wrought and AM samples are shown in Table 2. Despite the broader range of HV measurements in the AM samples, indicating a higher variability, the average did not differ significantly from the HV of wrought samples ($p = 0.744$).

PIP testing was used to determine the YS and UTS for both wrought and AM as shown in Table 3. For PIP, YS and UTS were significantly higher in the wrought samples (1028 ± 45.0 MPa, 1112 ± 32.0 MPa, respectively) than in the AM samples (972 ± 51.8 MPa: $p = 6.3*10^{-4}$, 1059 ± 59.0 MPa: $p = 1.1*10^{-4}$, respectively).

3.2. Material strength comparison from PIP and tensile tests

Fig. 1 shows a comparison of the YS and UTS derived from the PIP and tensile tests for all wrought and AM Ti6Al4V samples, including those later identified as outliers that were excluded from further analysis. For the AM samples, only UTS exhibited a significant difference between the two test methods ($p = 0.034$) while both YS and UTS were significantly different between the two tests for the wrought samples (YS: $p = 0.014$, UTS: $p = 0.0003$).

3.3. Tensile strength, PIP-derived strength, and microhardness relationships

To assess the sensitivity of the PIP test in predicting the YS and UTS, each outcome was compared with the results from the tension test to determine the mean absolute percentage error (MAPE), minimum, maximum, and average differences between them (Table 4). The MAPE and average difference for both AM and wrought YS were generally higher than their corresponding UTSs. The minimum differences, on the other hand, were similar except for wrought YS that exhibited the least difference of 0.3 MPa.

The general trends of the PIP-derived strength and HV were compared with the tensile test strength outcomes by sorting the tensile test results in ascending order (Fig. 2) for a visualization of how the three measurements values trend relative to each other. The comparison revealed that the PIP–derived UTS generally aligned better with the trend observed in the tensile–UTS than the tensile–YS for both wrought

Table 2
Vickers hardness of annealed wrought and PBF-LB AM Ti6Al4V.

Specimen Cohorts	Hardness (HV)	
	Mean ± SD	Range
Wrought (n = 25)	358 ± 17.1	326 – 389
AM HIP (n = 26)	360 ± 24.8	329 – 411

Table 1
Mechanical properties of annealed wrought and PBF-LB AM Ti6Al4V samples from tensile testing.

Specimen Cohorts	Modulus (GPa)		0.2% Yield (MPa)		UTS (MPa)	
	Mean ± SD	Range	Mean ± SD	Range	Mean ± SD	Range
Wrought (n = 25)	117 ± 7.3	100 – 131	1000 ± 39.4	951 – 1081	1081 ± 40.9	1036 – 1174
AM HIP (n = 26)	135 ± 10.6	118 – 159	942 ± 66.3	836 – 1074	1026 ± 48.1	951 – 1138

Table 3
Mechanical properties of annealed wrought and PBF-LB AM Ti6Al4V samples from PIP testing.

Specimen Cohorts	0.2% Yield (MPa)		UTS (MPa)	
	Mean ± SD	Range	Mean ± SD	Range
Wrought (n = 25)	1028 ± 45.0	952 – 1109	1112 ± 32.0	1068 – 1177
AM HIP (n = 26)	972 ± 51.8	872 – 1043	1059 ± 59.0	961 – 1213

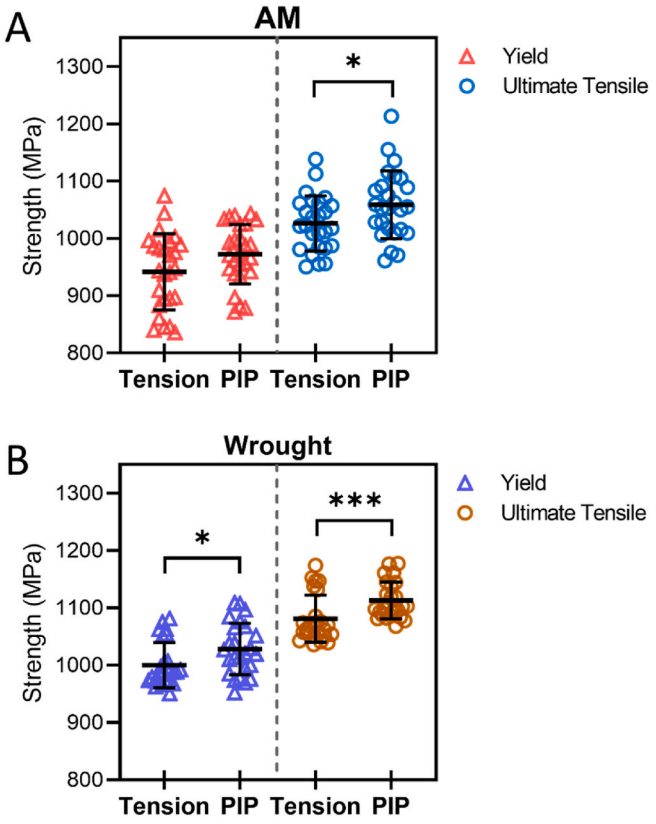

Fig. 1. Scatter plot comparing the yield and ultimate tensile strength of AM (A) and wrought (B) Ti6Al4V samples from PIP and Tensile tests. The mean and standard deviation are shown for each set of data.

Table 4
Mean Absolute Percentage Error (MAPE), minimum difference, average difference, and maximum difference between PIP and Tensile testing for yield strength (YS) and Ultimate Tensile Strength (UTS) for AM and Wrought.

	MAPE (%)	Min Difference (MPa)	Average Difference (MPa)	Max Difference (MPa)
AM YS	3.7	1.2	36.0	68.7
AM UTS	3.2	1.2	33.9	100.3
Wrought YS	4.2	0.3	41.1	109.9
Wrought UTS	3.0	1.7	32.0	66.9

and AM samples. These observations were reflected in the coefficients of determination (r^2) obtained from linear regressions of PIP-derived strength against tensile test strength, omitting five samples showing significant anisotropy. There was a stronger positive linear relationship for UTS (AM: $r^2 = 0.85$, wrought: $r^2 = 0.84$) (Figs. 3B and 4B) between the PIP and tensile results than for YS (AM: $r^2 = 0.48$, wrought: $r^2 = 0.22$) (Figs. 3A and 4A).

Regarding the relationship between the HV and the tensile test strength outcomes, the microhardness of AM samples trended similarly for both YS and UTS (Fig. 2A and B). This trend was less obvious for the wrought samples (Fig. 2C and D). Correspondingly, the positive linear correlations were stronger in the AM samples (YS: $r^2 = 0.59$, UTS: $r^2 = 0.70$) (Fig. 3C and D) than in the wrought (YS: $r^2 = 0.14$, UTS: $r^2 = 0.17$) (Fig. 4C and D).

The 95% confidence and prediction intervals were plotted alongside the linear models predicting tensile measurements from both PIP and HV in Figs. 3 and 4. The confidence intervals take into account the uncertainty in model parameter estimation. However, prediction intervals are used to predict a future measurement; even if the true YS or UTS were known, there would still be uncertainty about the exact value produced by a tensile test. Prediction intervals take into account multiple sources of error and as a result are wider than confidence intervals. They are also wider than the typical variation found in tensile measurements, since they have to account for the uncertainty caused by unmeasured confounding factors such as manufacturing methods alongside measurement error and model parameter estimation.

The exact width of confidence and prediction intervals vary across the range being measured. However, to provide an indication of their widths, interval widths were calculated at the values obtained for samples chosen to have the median YS value as measured by tensile testing and reported in Table 5.

3.4. Anisotropy in AM Ti6Al4V

To determine whether different manufacturing processes result in variability that confounds the correlation between the two tests, a PIP assessment of anisotropy was performed on two sample groups: 3 samples with XY-plane PIP tests that significantly diverged from the tensile testing from one manufacturer, and 3 others that showed good correlation with between tensile testing and PIP tests performed in the XY-plane (Fig. 5) from a range of other manufacturers. Further PIP testing was performed in a plane orthogonal to the build direction (the XZ-plane), 45° from the build direction, and 135° from the build direction. Anisotropy was then characterized by examining differences in scanned profiles aligned parallel and perpendicular to the build direction. Samples characterized to have higher levels of anisotropy exhibited lower correlation with tensile measured properties, while those characterized to have lower levels of anisotropy exhibited improved correlation with tensile measured properties.

Samples showing stronger anisotropy were identified as weaker in the Z-direction (the tensile axis) than other directions. This can be seen in Fig. 5 where the Z-direction residual indent profiles show higher pile up height (32 μm) compared with the X-direction (17 μm) for these samples (left column) with a 16 μm difference in pile up height. Three other samples were investigated as a control and found to have a smaller difference between pile up height in the X and Z directions of 8 μm, indicating a lower degree of radial asymmetry and corresponding lower level of anisotropy. PIP tests create a 3-dimensional stress state, influenced by material behavior in all directions. It is therefore expected that PIP will overestimate material strength compared with a tensile test aligned with a weaker direction.

3.5. The impact of oxygen content

To assess the relative influence of oxygen content on tensile measurements, the correlations between the tensile YS and tensile UTS for the AM and wrought Ti6Al4V were examined (Fig. 6). For the tensile test results, the AM samples showed a stronger correlation with the oxygen content (YS: $r = 0.66$, UTS: $r = 0.68$) than the wrought samples (YS: $r = 0.14$, UTS: $r = 0.48$). Overall, using oxygen content as a predictor in the linear model regression did not significantly improve the fit between PIP and tensile measurements of both YS and UTS. Oxygen content improved only two model fits which were: predicting YS from PIP for AM ($p = 0.0004$) and predicting UTS from PIP for wrought samples ($p = 0.009$).

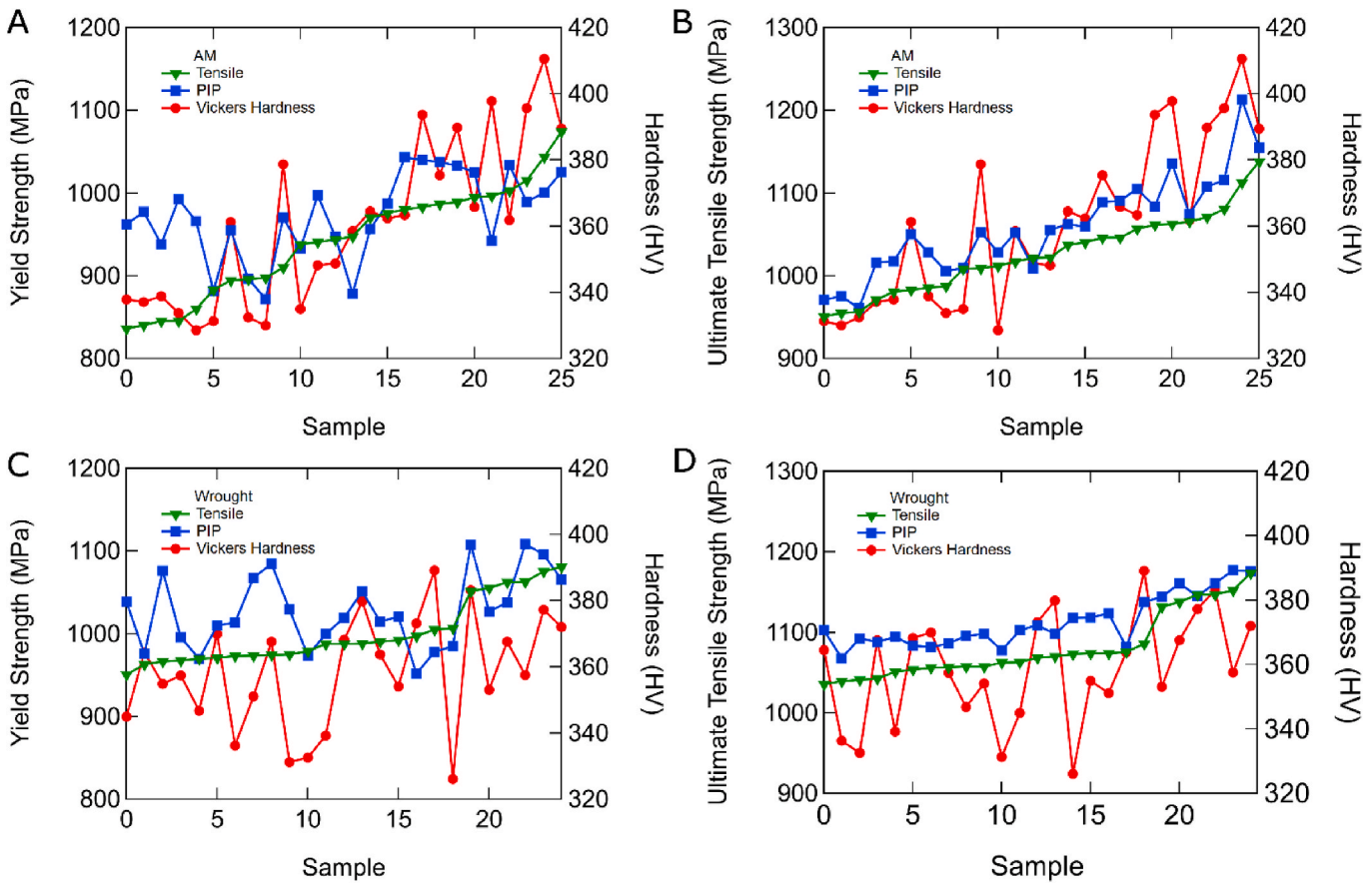

Fig. 2. Comparison of tensile, PIP, and Vickers Hardness test trends for yield strength (YS) (A, C) and ultimate tensile strength (B, D) of the AM (A, B) and for Wrought (C, D) samples.

4. Discussion

Additive manufacturing is now widely utilized in the production of orthopedic medical devices; however, due to the numerous variables involved in the process, it requires a thorough understanding of how mechanical properties are affected by changes in processing conditions. Given the vast range of processing conditions, fabricating tensile test coupons to represent process combinations to determine the impact on mechanical properties can be impractical. Hardness testing, which requires less time and resources, can be beneficial in estimating material strength properties. However, predicting strength based solely on hardness measurements can be challenging for materials that exhibit work-hardening behavior, such as Ti6Al4V (Southern et al., 2023). The PIP method, although similar to hardness testing, also incorporates iterative FEM modeling to derive material strength. This study utilized the PIP test to derive the YS and UTS of wrought and PBF-LB AM Ti6Al4V. The PIP results were compared with the strength information obtained from tensile testing of the same specimens to determine the level of accuracy of the PIP method and to identify any possible correlations between the two methods.

From the tensile testing, differences were observed in all the mechanical properties between the wrought and AM Ti6Al4V samples. The relatively higher YS and UTS of wrought (1000 and 1080 MPa) samples compared with the AM (942 and 1026 MPa) are consistent with previous observations (Sterling et al., 2016). Research has shown that the presence of residual internal defects, even after applying the HIP post-processing treatment to the AM Ti6Al4V, could influence the YS and UTS in this way (de et al., 2023; Kobryn and Semiatin, 2001; Bartolomeu et al., 2016; Gaytan et al., 2009). It appears that the strength of AM materials becomes comparable to or exceeds the strength of wrought samples when internal defects are drastically minimized (Fousova et al., 2018), although other microstructural factors such as grain size and relative alpha-beta phase levels are important to consider.

Despite the differences observed in the tensile properties between the wrought and AM samples, the average microhardness results were similar for both materials. However, the extent of variability in AM samples exceeded that of the wrought. This is similar to what others have observed (Longhitano et al., 2018; Keist and Palmer, 2017; Dolev et al., 2021). An example is Keist et al.'s study that reported a wide range of hardness measurements within the same area of electron beam-based directed energy deposition (DED) samples, varying from 2.85 to 3.41 GPa (Keist and Palmer, 2017). The wide variation in hardness of Ti6Al4V has been associated with strain rate sensitivity, indentation size effect when very fine scale measurement techniques are used, and variations in build location (Longhitano et al., 2018; Özerinç et al., 2021; Hu et al., 2020). Additionally, the differences in the microstructural composition of the samples resulting from different heat treatments could potentially impact their hardness. Murr et al. reported a good agreement between the microstructure, specifically the average alpha plate dimensions, and the hardness of Ti6Al4V cylindrical specimens (Murr et al., 2009). Dietrich et al. also reported a decrease in the tensile strength and hardness due to an increase in the beta phase of PBF-LB Ti6Al4V samples that underwent the HIP process (Dietrich et al., 2020). Similarly, the AM samples in this study underwent HIP post-processing treatment and exhibited lower tensile strength compared with the annealed wrought counterparts. Although a reduction in hardness was not apparent in this study.

Coefficients of determination are used to compare the two indentation methods' ability to predict mechanical properties as measured by tensile testing. PIP shows a higher coefficient of determination for YS

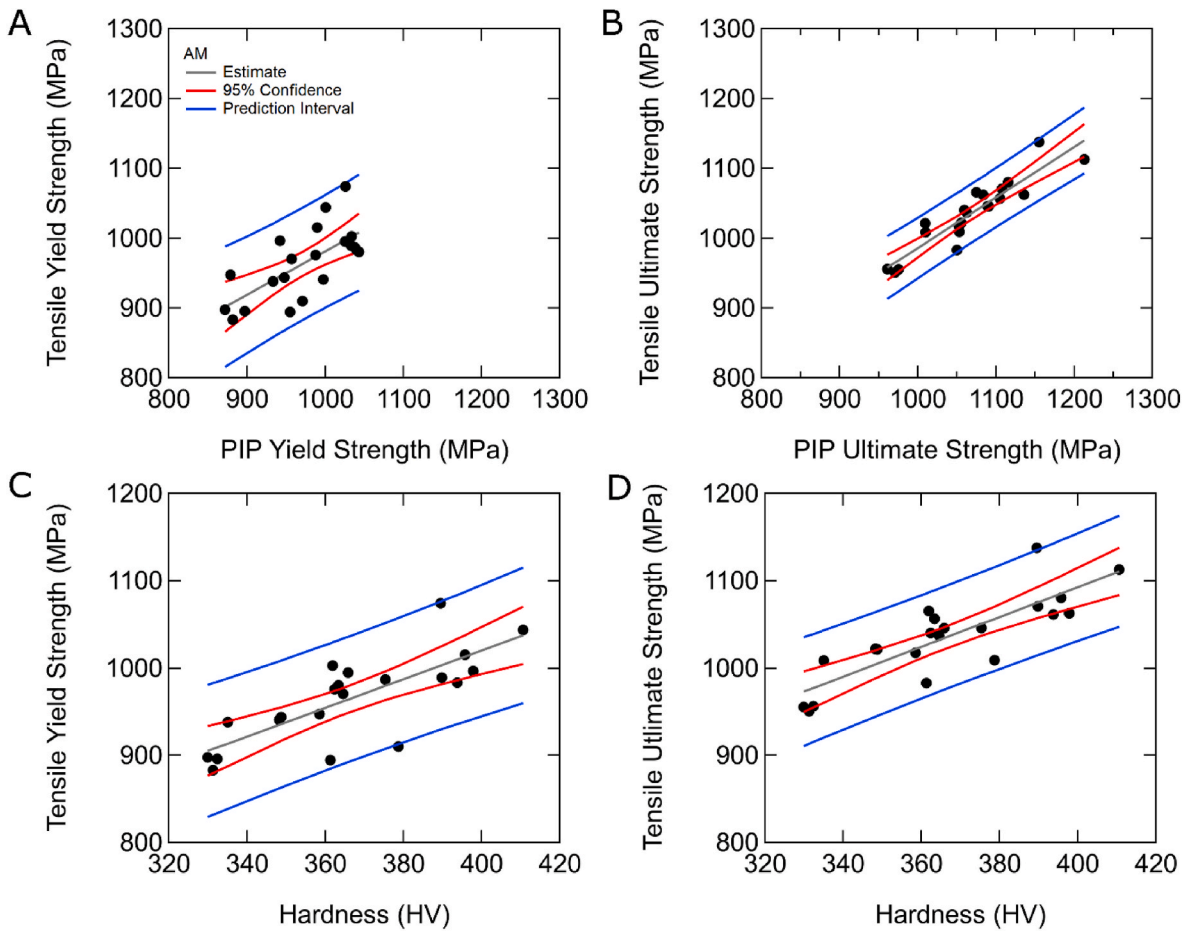

Fig. 3. Confidence and Prediction Intervals for the AM samples when comparing PIP YS to Tensile YS (A), PIP UTS to Tensile UTS (B), Vickers Hardness to Tensile YS (C) and Vickers Hardness to Tensile UTS (D). The red band represents the 95% confidence interval and the blue represents the prediction interval. (For interpretation of the references to colour in this figure legend, the reader is referred to the Web version of this article.)

and UTS of wrought and UTS of AM materials than HV indicating a better predicter of tensile measured values. The coefficient of determination is only higher for HV in the case of AM YS, where the two values remain close (0.59 and 0.48 respectively). Previous work has reported a similar strong linear correlation between the strength and HV of AM Ti6Al4V (Keist and Palmer, 2017). The analysis above focuses on obtaining the best possible estimate of tensile testing based on PIP and HV values. For AM build verification, it may be preferable to take a conservative approach which incorporates the uncertainty in measurement error and unmeasured factors to produce a threshold below which it is very unlikely that the tensile measurement will fall. This is done here using prediction intervals. The expected tensile measurement can be predicted using the regression model, and then half the width of the 95% prediction interval subtracted from it, equivalent to using the lower bound of the prediction interval. The tensile measurement for the sample will be higher than this estimate with 97.5% confidence (Pietrasik et al., 2025).

The accuracy of the indentation results was hindered in part by the observed anisotropy of some of the AM samples that displayed a more substantial deviation from the tensile results. The impact of anisotropy demonstrated in this study confirms an additional factor that poses challenges to the proposed prediction approach for the strain-rate sensitive Ti6Al4V. Anisotropy arises from the nature of the underlying microstructure, which is typically dictated by the adopted manufacturing process (Longhitano et al., 2018; Keist and Palmer, 2017). Sterling et al. attributed anisotropy in DED Ti6Al4V parts to high localized heating and cooling rates during processing (Sterling et al., 2016). It can be inferred that the AM samples in this study, manufactured via PBF using parameters such as scan spacing, scan speed, and laser or electron beam spot size, exhibited anisotropy, also as a consequence of the AM process (Bartolomeu et al., 2016). Anisotropy in AM samples is inevitable to some extent due to the directionality of the process and the increased likelihood of local variations during powder consolidation.

Anisotropy can have a pronounced impact on comparisons of hardness and PIP tests to uniaxial tensile testing as they are influenced by material properties in all directions (Poondla et al., 2009). Thus, it is expected that predicted properties would lie between tensile values measured in different directions. In this work, all tensile testing was performed with the loading axis parallel to the build direction, providing no information about any anisotropy present in the samples. To investigate the potential for anisotropy causing a discrepancy between indentation methods and tensile testing, additional PIP indents were performed perpendicular to the build direction in three samples that showed high deviation between PIP and tensile testing, as well as three samples with low mean absolute errors between the two methods. This testing revealed two important takeaways. Firstly, the samples with higher deviations (i.e., those with lower tensile measured YS) showed stronger anisotropy than their counterparts. These samples were also found to be softer in the build direction compared with the in-plane directions. This suggests that the tensile test measured properties along an orientation with lower YS compared with the value predicted by indentation, which includes contributions from all directions. Secondly, this finding also suggests that the HIP post-processing treatment did not fully eliminate as-built anisotropy as intended.

Unsurprisingly, there was a linear positive relationship between the

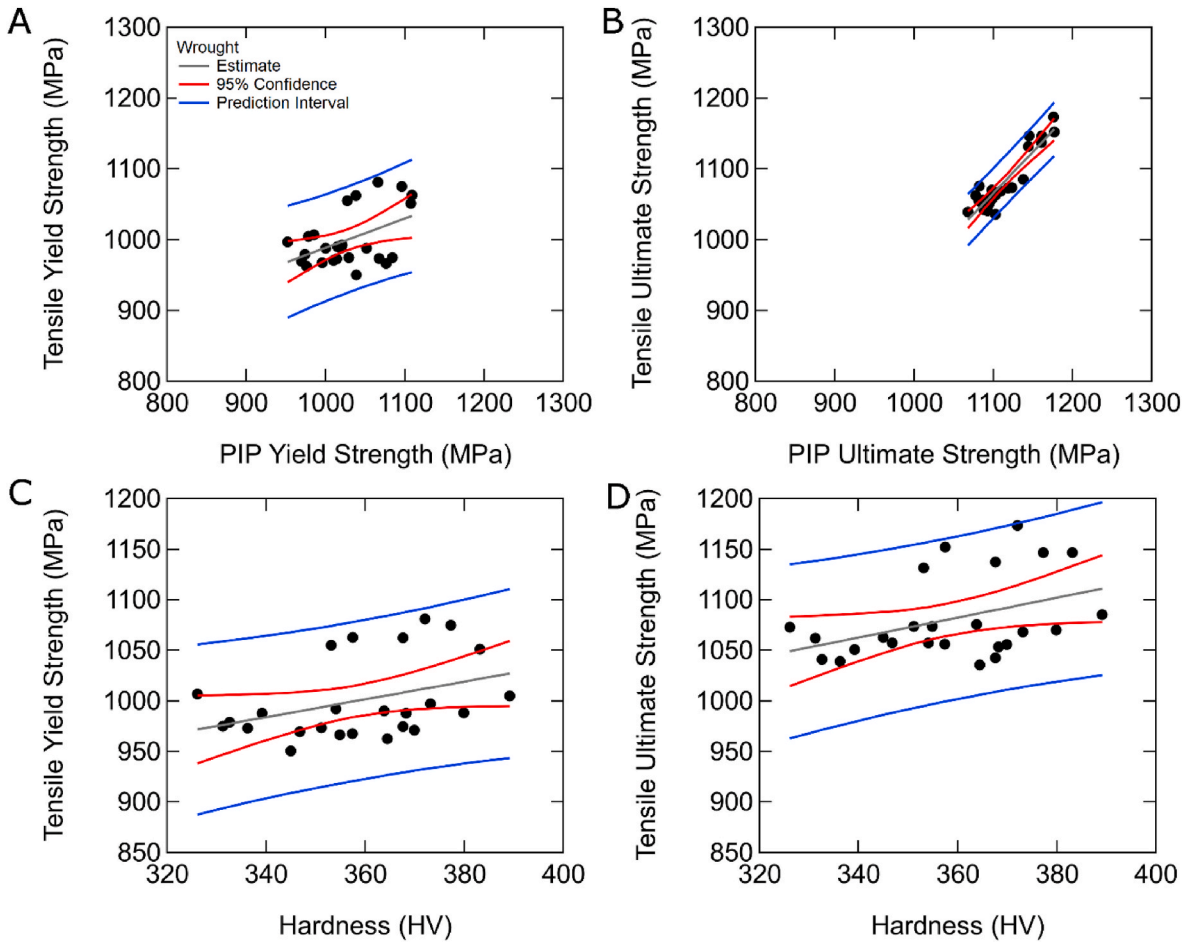

Fig. 4. Confidence and Prediction Intervals n for the Wrought samples when comparing PIP YS to Tensile YS (A), PIP UTS to Tensile UTS (B), Vickers Hardness to Tensile YS (C) and Vickers Hardness to Tensile UTS (D). The red band represents the 95% confidence interval and the blue represents the prediction interval. (For interpretation of the references to colour in this figure legend, the reader is referred to the Web version of this article.)

Table 5
Two-sided 95% confidence and 95% prediction interval widths for models of tensile results from PIP and Vickers hardness testing for yield strength (YS) and Ultimate Tensile Strength (UTS) for AM and Wrought for samples with median YS values.

	PIP 95% Confidence Interval Width (MPa)	PIP 95% Prediction Interval Width (MPa)	Vickers hardness 95% Confidence Interval Width (MPa)	Vickers hardness 95% Prediction Interval Width (MPa)
AM YS	35.3	161.1	31.1	143.7
AM UTS	18.2	84.3	25.6	118.2
Wrought YS	29.9	150.0	35.7	158.2
Wrought UTS	18.8	71.3	36.5	161.9

oxygen content and the measured strength of the AM Ti6Al4V from the tensile test. Since the model fit between PIP and tensile measurements did not significantly improve with the use of oxygen content as a predictor overall, it is suspected that the oxygen content will most likely correlate with unmeasured potential factors that cause variability. Interestingly, the influence of oxygen content was less pronounced in the wrought Ti6Al4V. The presence of oxygen affects both wrought and AM Ti6Al4V similarly by increasing strength and hardness, while potentially reducing ductility (Gardner et al., 2021; Haden et al., 2015). Nonetheless, the extent of this impact may differ owing to differences in their manufacturing process. Unlike the wrought, the usual practice of multiple powder reuse during the manufacturing of AM Ti6Al4V increases oxygen uptake and exacerbates the unpredictable increase in strength outcome. The impact of oxygen on Ti6Al4V strength becomes noticeable at concentrations above 0.2 wt% (Gardner et al., 2021; Standard Specification for Wrought Titanium, 2023; Standard Specification for Additive Manufacturing, 2014).

The use of a large indenter has been suggested as a means of improving the accuracy of the PIP method by capturing a larger variety of grains or microconstituents in underlying microstructures (Tang et al., 2021). Ozerinc et al. reported a strong indentation size effect in Ti6Al4V specimens after characterizing with microhardness, nanoindentation, micropillar compression, and micro-scratch testing. Their results showed that hardness increased with a decrease in the indentation depth, leading to an overestimation of the macroscopic mechanical properties (Özerinç et al., 2021). However, we do not anticipate any indentation size effect in this study due to the use of a 0.5 mm spherical indenter, which is large enough to capture multiple grains and grain boundaries in the microstructure. This study, as well as past reports, imply that the accuracy of the PIP test in predicting material strength appears to rely on the evidence of isotropy, such as observations of radial symmetry of indents during testing (Southern et al., 2023). Therefore, one should exercise increased caution when implementing this method for potentially anisotropic materials, such as the AM Ti6Al4V samples. While PIP can be used to confirm the presence of anisotropy in a material (Fig. 5), it would be preferable to modify the post-processing of the AM material to reduce anisotropy before using

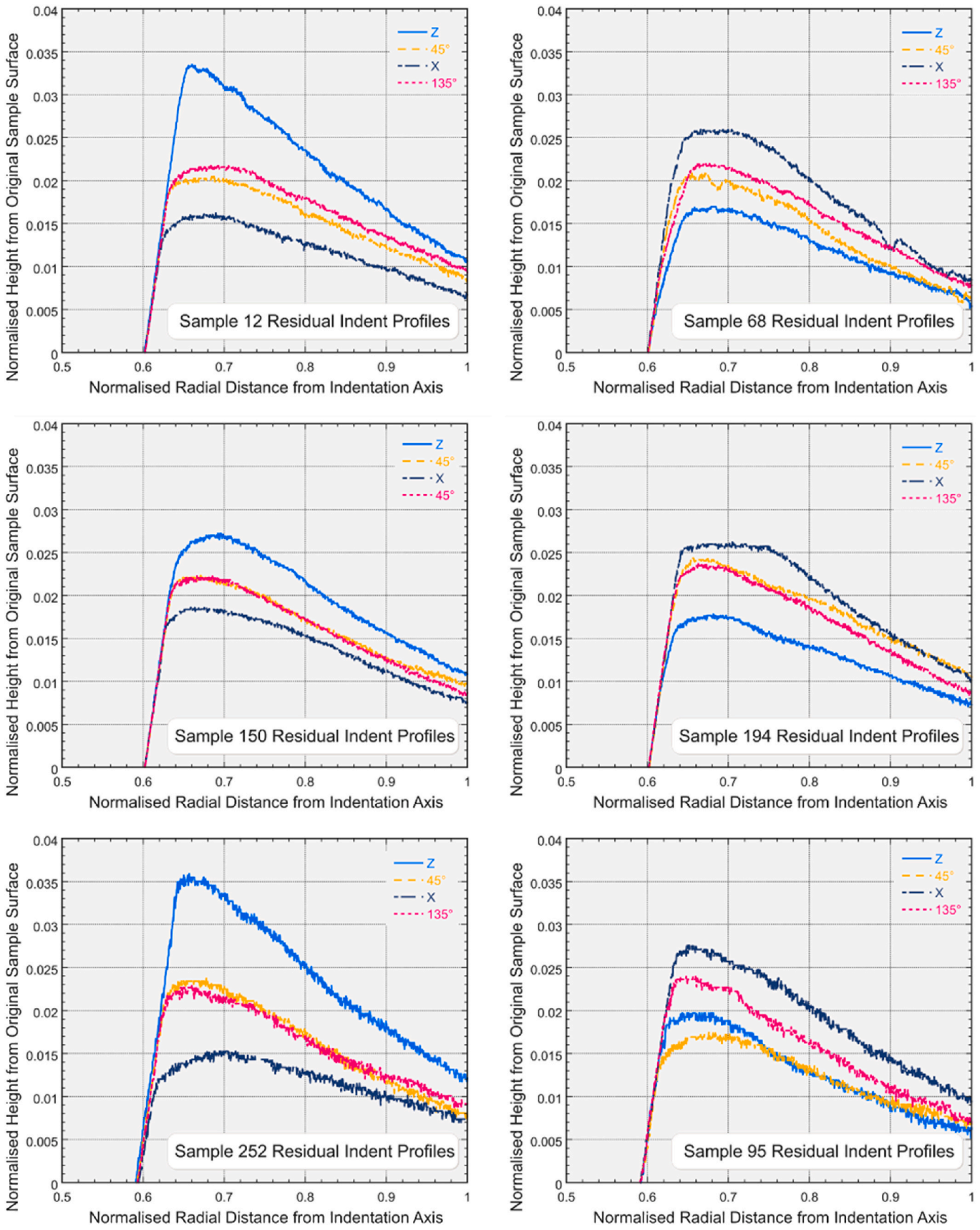

Fig. 5. Residual indent profiles from indents into the XZ-plane showing high anisotropy in samples where correlation with tensile was lower (left), compared with more isotropic samples that exhibited increased correlation with tensile (right).

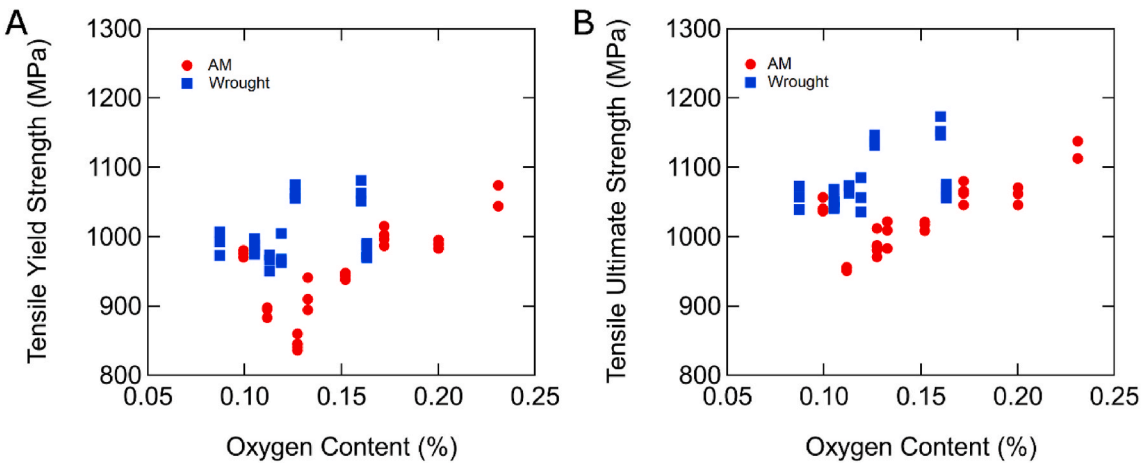

Fig. 6. Correlation of yield strength (A) and ultimate tensile strength (B) as determined by tensile testing to oxygen content for the AM and Wrought samples.

PIP as the verification method. Identifying the impact of anisotropy can be beneficial for further improvement and validation of the PIP method for future material strength predictions. Differences in strain-rate between the different methods of testing can also influence the comparison between the techniques (McKeown et al., 2025) as well as the values themselves of mechanical properties. McKeown et al. showed a reduction in tensile yield stress of 40-50 MPa with a reduction in strain rate from 10^{-2} s^{-1} to 10^{-4} s^{-1}. Complications arise when determining a single strain rate from indentation at a given indentation velocity due to the complex nature of the stress-state under the indenter, although McKeown et al. observed a reduction of PIP YS of 90-100 MPa with a reduction in indenter velocity from 3 μm s^{-1} to 0.3 μm s^{-1}. This underscores the need for properly considering both the indentation and tensile strain rates when validating one test method against another. The PIP method can be used as a faster approach to identifying the effect of different strain rate on a material's mechanical property.

One of the limitations of this study is that anisotropy was assessed in only a few AM samples. Including both wrought and AM samples would have provided a comprehensive comparison of the two materials. Additionally, a thorough microstructural analysis of both materials could have better confirmed and provided bases for comparing the extent of their anisotropy. Despite these limitations, the study successfully demonstrated the relationship and feasibility of the PIP test in predicting the tensile mechanical properties. Future studies could explore the impact of varied indentation size, shape, and rate on AM anisotropic materials, along with a deeper investigation into the underlying microstructure. Since oxygen content did not influence the relationship between the PIP and tensile results, it appears that incorporating oxygen content predictions during validation processes may not be necessary. However, further exploration using larger datasets may prove otherwise.

5. Conclusions

In this study the results from two indentation methods (Vickers microhardness and PIP) were compared to the results of tensile testing from a range of additively manufactured and wrought titanium samples to assess the viability of the indentation methods for build verification purposes. The study found:

- The average microhardness values were similar for wrought and AM Ti6Al4V, but the latter showed a wider variability.
- The PIP method was used to derive the strength (YS and UTS) of wrought and AM Ti6Al4V, and positive correlations were found between the PIP-derived strength and the tensile strength outcomes, but up to varying degrees of accuracy.
- Indentation-based predictions are influenced by material behavior in all directions. For strongly anisotropic samples, this causes differences between indentation inferred properties and those measured by a uniaxial tensile test.
- The PIP method presented lower mean absolute percentage errors of UTS 3.0% and 3.2% for wrought and AM Ti6Al4V, compared with the YS (4.1%, 3.7% respectively).
- Prediction interval widths have shown PIP to be a better predictor of tensile values than HV for YS and UTS of wrought materials and UTS of AM materials. HV provided a better model for YS of AM materials, although the two techniques behaved similarly.
- Consideration should be given to the effects of anisotropy and strain-rate sensitivity for materials like AM Ti6Al4V when implementing PIP for build verification.
- Finally, the oxygen content correlated strongly with strength in the AM Ti6Al4V for the tensile test in this study, but the effect was less pronounced in the wrought samples, possibly due to their lower oxygen levels.

These results indicate that, with sufficient validation including attention to: sample anisotropy, indentation parameters, and strain rate; indentation techniques could be utilized in future AM build verification testing.

CRediT authorship contribution statement

Abigail Tetteh: Formal analysis, Investigation, Writing – original draft. **Daniel Porter:** Formal analysis, Funding acquisition, Investigation, Writing – review & editing. **Thomas Southern:** Formal analysis, Investigation, Writing – review & editing. **Jimmy Campbell:** Formal analysis, Investigation, Writing – review & editing. **Mary Fortune:** Formal analysis, Writing – review & editing. **Matthew Di Prima:** Conceptualization, Formal analysis, Funding acquisition, Investigation, Writing – original draft, Writing – review & editing.

Declaration of competing interest

The authors declare that they have no known competing financial interests or personal relationships that could have appeared to influence the work reported in this paper.

Acknowledgments

This research was also supported in part by an appointment to the Research Participation Program at the U.S. FDA administered by the Oak Ridge Institute for Science and Education (ORISE) through an

interagency agreement between the U.S. Department of Energy and FDA. J Campbell would like to acknowledge the support from UKRI in the form of a Future Leaders Fellowship grant (MR/W01338X/1).

None of the authors have a conflict of interest to report. The findings and conclusions in this article have not been formally disseminated by the U.S. FDA and should not be construed to represent any agency determination or policy. The mention of commercial products, their sources, or their use in connection with material reported herein is not to be construed as either an actual or implied endorsement of such products by the Department of Health and Human Services.

Appendix A. Supplementary data

Supplementary data to this article can be found online at https://doi.org/10.1016/j.jmbbm.2026.107507.

Data availability

Data will be made available on request.

References

Additive manufacturing — general principles — fundamentals and vocabulary, ASTM. Annu. Book ASTM Stand., 2021

Bartolomeu, F., et al., 2016. Predictive models for physical and mechanical properties of Ti6Al4V produced by selective laser Melting. Mater. Sci. Eng., A 663, 181–192.

Cahoon, J., Broughton, W., Kutzak, A., 1971. The determination of yield strength from hardness measurements. Metall. Trans. A 2, 1979–1983.

Collins, P., Welk, B., Searles, T., Tiley, J., Russ, J., Fraser, H., 2009. Development of methods for the quantification of microstructural features in α+ β-processed α/β titanium alloys. Mater. Sci. Eng., A 508 (1–2), 174–182.

de Formanoir, C., Logé, R.E., 2023. Postprocess treatments for surface quality improvement, mitigation of defects, and microstructural control. In: Quality Analysis of Additively Manufactured Metals, pp. 261–320.

Dietrich, K., Diller, J., Dubiez-Le Goff, S., Bauer, D., Forêt, P., Witt, G., 2020. The influence of oxygen on the chemical composition and mechanical properties of Ti-6Al-4V during laser powder bed fusion (L-PBF). Addit. Manuf. 32, 100980.

Dolev, O., Osovski, S., Shirizly, A., 2021. Ti-6Al-4V hybrid structure mechanical properties—Wrought and additive manufactured powder-bed material. Addit. Manuf. 37, 101657.

Elias, C., Lima, J., Valiev, R., Meyers, M., 2008. Biomedical applications of titanium and its alloys. Jom 60, 46–49.

Faraway, J.J., 2002. Practical Regression and ANOVA Using R. University of Bath Bath.

Fogarasi, M., Snodderly, K.L., Di Prima, M.A., 2023. A survey of additive manufacturing trends for FDA-Cleared medical devices. Nat. Rev. Bioeng. 1 (10), 687–689.

Fousova, M., Vojtech, D., Doubrava, K., Daniel, M., Lin, C.F., 2018. Influence of inherent surface and internal defects on mechanical properties of additively manufactured Ti6Al4V alloy: comparison between selective laser melting and electron beam melting. Materials 11 (4). https://doi.org/10.3390/ma11040537.

Gardner, H., et al., 2021. Quantifying the effect of oxygen on micro-mechanical properties of a near-alpha titanium alloy. J. Mater. Res. 1–16.

Gaytan, S.M., Murr, L.E., Medina, F., Martinez, E., Lopez, M., Wicker, R.B., 2009. Advanced metal powder based manufacturing of complex components by electron beam melting. Mater. Technol. 24 (3), 180–190.

Haden, C., Collins, P., Harlow, D., 2015. Yield strength prediction of titanium alloys. Jom 67, 1357–1361.

Hernandez-Nava, E., Mahoney, P., Smith, C.J., Donoghue, J., Todd, I., Tammas-Williams, S., 2019. Additive manufacturing titanium components with isotropic or graded properties by hybrid electron beam melting/hot isostatic pressing powder processing. Sci. Rep. 9 (1), 4070. https://doi.org/10.1038/s41598-019-40722-3.

Hooreweder, B.V.. Overview of LPBF parameters. no date. [Online]. Available: https://www.futurelearn.com/info/courses/laser-powder-bed-fusion-process-parameters-and-parameter-optimization/0/steps/259833.

Hu, H., Xu, Z., Dou, W., Huang, F., 2020. Effects of strain rate and stress state on mechanical properties of Ti-6Al-4V alloy. Int. J. Impact Eng. 145. https://doi.org/10.1016/j.ijimpeng.2020.103689.

Karolewska, K., Ligaj, B., Boronski, D., 2020. Strain analysis of Ti6Al4V titanium alloy samples using digital image correlation. Materials 13 (15). https://doi.org/10.3390/ma13153398.

Kaur, M., Singh, K., 2019. Review on titanium and titanium based alloys as biomaterials for orthopaedic applications. Mater. Sci. Eng., C 102, 844–862. https://doi.org/10.1016/j.msec.2019.04.064.

Keist, J.S., Palmer, T.A., 2017. Development of strength-hardness relationships in additively manufactured titanium alloys. Mater. Sci. Eng., A 693, 214–224.

Kobryn, P., Semiatin, S., 2001. Mechanical Properties of laser-deposited Ti-6Al-4V.

Lai, M., Lim, K., 1991. On the prediction of tensile properties from hardness tests. J. Mater. Sci. 26, 2031–2036.

Lincoln, J.E., 2012. Overview of the us fda gmps: good manufacturing practice (gmp)/quality system (qs) regulation (21 CFR part 820). J. Validation Technol. 18 (3), 17.

Longhitano, G.A., Larosa, M.A., Jardini, A.L., de Carvalho Zavaglia, C.A., Ierardi, M.C.F., 2018. Correlation between microstructures and mechanical properties under tensile and compression tests of heat-treated Ti-6Al–4 V ELI alloy produced by additive manufacturing for biomedical applications. J. Mater. Process. Technol. 252, 202–210.

McKeown, P.J., Miller, J.R., Clyne, T.W., 2025. Effects of creep in titanium at room temperature during tensile and profilometry-based indentation plastometry testing. Adv. Eng. Mater. 27 (9), 2402645.

Murr, L., et al., 2009. Microstructures and mechanical properties of electron beam-rapid manufactured Ti–6Al–4V biomedical prototypes compared to wrought Ti–6Al–4V. Mater. Charact. 60 (2), 96–105.

Pietrasik, M., et al., 2025. Capturing variability in material property predictions for plastics recycling via machine learning. Digit. Chem. Eng., 100239

Poondla, N., Srivatsan, T.S., Patnaik, A., Petraroli, M., 2009. A study of the microstructure and hardness of two titanium alloys: commercially pure and Ti–6Al–4V. J. Alloys Compd. 486 (1–2), 162–167.

Radlof, W., Benz, C., Heyer, H., Sander, M., 2020. Monotonic and fatigue behavior of EBM manufactured Ti-6Al-4V solid samples: experimental, analytical and numerical investigations. Materials 13 (20). https://doi.org/10.3390/ma13204642.

Schwalbach, E.J., et al., 2022. Effects of local processing parameters on microstructure, texture, and mechanical properties of electron beam powder bed fusion manufactured Ti–6Al–4V. Mater. Sci. Eng., A 855, 143853.

Southern, T., Campbell, J., Fang, C., Nemcova, A., Bannister, A., Clyne, T., 2023. Use of hardness, PIP and tensile testing to obtain stress-strain relationships for metals. Mech. Mater. 187, 104846.

Southern, T., Kircher, R., Meyer, A., Campbell, J., 2024. Accelerated qualification of Ti-6Al-4V medical implants using profilometry-based indentation plastometry. In: Presented at the International Conference on Additive Manufacturing, Atlanta, GA.

Standard Specification for Additive Manufacturing Titanium-6 Aluminum-4 Vanadium with Powder Bed Fusion, 2014. ASTM.

Standard Specification for Wrought Titanium-6Aluminum-4Vanadium Alloy for Surgical Implant Applications, 2023. ASTM.

Standard Test Method for Determination of Oxygen and Nitrogen in Titanium and Titanium Alloys by Inert Gas Fusion, 2013. ASTM.

Standard Test Methods for Tension Testing of Metallic Materials, 2016. ASTM.

Standard Test Methods for Vickers Hardness and Knoop Hardness of Metallic Materials, 2023. ASTM.

Sterling, A.J., Torries, B., Shamsaei, N., Thompson, S.M., Seely, D.W., 2016. Fatigue behavior and failure mechanisms of direct laser deposited Ti–6Al–4V. Mater. Sci. Eng., A 655, 100–112. https://doi.org/10.1016/j.msea.2015.12.026.

Tabor, D., 1951. The hardness and strength of metals. J. Inst. Met. 79, 1.

Tang, Y.T., Campbell, J.E., Burley, M., Dean, J., Reed, R., Clyne, T., 2021. Profilometry-based indentation plastometry to obtain stress-strain curves from anisotropic superalloy components made by additive manufacturing. Materialia 15, 101017.

Tekkaya, A.E., 2001. Improved relationship between vickers hardness and yield stress for cold formed materials. Steel Res. 72 (8), 304–310.

Özerinç, S., et al., 2021. Micromechanical characterization of additively manufactured Ti-6Al-4V parts produced by electron beam melting. Jom 73 (10), 3021–3033. https://doi.org/10.1007/s11837-021-04804-w.